Journal of Fluorine Chemistry 235 (2020) 109546

Contents lists available at ScienceDirect

Journal of Fluorine Chemistry

journal homepage: www.elsevier.com/locate/fluor

Study on micro-structure and transport properties of KF-NaF-AlF_3-Al_2O_3 system by first-principles molecular dynamics simulation

Hui Guo[a], Jie Li[a], Hongliang Zhang[a,*], Jiawei Luo[a], Jingkun Wang[a], Chunling Mou[b], Shangyuan Wu[a], Chuanxin Zong[a]

[a] School of Metallurgy and Environment, Central South University, Changsha 410083, China
[b] Hongqiao Group Limited, Huixian First Road, Zouping Economic Development Zone, Zouping City 256200, Shandong Province, China

ARTICLE INFO

Keywords:
KF-NaF-AlF_3-Al_2O_3
Micro-structure
Transport properties
First-principles molecular dynamics

ABSTRACT

It has always been a challenging problem to conduct research on low temperature aluminum electrolyte KF-NaF-AlF_3-Al_2O_3 because of high temperature and strong corrosiveness in aluminum electrolysis industry. Fortunately, the rapid advancement of computational materials science provides us with a good tool to study it. In this paper, the ionic micro-structure and transport properties of KF-NaF-AlF_3-Al_2O_3 system are studied by adopting first-principles molecular dynamics simulation directly. The calculated results show that the complex ion groups in KF-NaF-AlF_3-Al_2O_3 system are mainly $[AlF_4]^-$, $[AlF_5]^{2-}$ and $[AlF_6]^{3-}$, meantime, with the increasing concentration of Al_2O_3, $[AlF_4]^-$ decreases but the coordination number of Al-F complex ion groups increases gradually. Intricate complex ion groups of Al-F-Al, Al-O-Al and Al-O-F are formed on account of the presence of bridge F and bridge O ions. Besides, the proportion of bridge F and Bridge O ions increases with the increasing concentration of Al_2O_3, and the ionic micro-structure of the system becomes more intricate than before, reducing the ionic conductivity and increasing the viscosity of the system. This study can provide a useful guide for designing suitable low temperature electrolyte system in aluminum electrolysis production.

1. Introduction

Electrolytic aluminum is a process with high energy consumption and serious environmental pollution. For more than 100 years, the electrolyte used in electrolytic aluminum has hardly changed, which is still dominated by NaF-AlF_3 system [1]. Traditional NaF-AlF_3 melt has a higher operating temperature, generally between 1223 − 1253 K, greatly increasing the energy consumption and CO_2 emission of electrolytic aluminum [2]. In recent years, researchers have tried to find a low temperature aluminum electrolyte to replace it and reduce the production cost of aluminum electrolysis. With lower liquidus temperature and better solubility of alumina than NaF-AlF_3 system [3], KF-NaF-AlF_3 system has been extensively studied by researchers [4–6]. While they mainly concentrated on some basic physical and chemical properties, such as melt density, liquidus temperature and ionic conductivity [3,4]. In our previous work and other research [7,8], the ionic structure, transport and electronic properties of KF-NaF-AlF_3 system has been analyzed, which neglected the dissolution of Al_2O_3 in the system so that it is not enough to know the real micro-structure and transport properties of KF-NaF-AlF_3-Al_2O_3 system.

With the development of Raman spectra [9], NMR [10] and computer simulation technology [11–13], great progress has been made in the research of high temperature melts in aluminum electrolyte. Compared with experimental methods, computer simulation technology has incomparable cost advantages. Furthermore, based on a certain physical model, it is a good method to study the structure and properties of aluminum electrolyte melt by interatomic potential molecular dynamics (IPMD) simulation [14,15]. However, IPMD method highly depends on potential function and potential parameters, and there is no suitable potential parameters for IPMD simulation of KF-NaF-AlF_3-Al_2O_3 system currently. Fortunately, with the rapid advancement of computer computing speed, it is possible to calculate properties of materials directly from first-principles. Since Car and Parrinello [16] proposed first-principles molecular dynamics(FPMD) simulation method in 1985, it has been well applied to KCl-LiCl [17–20], NaF-AlF_3 [21] and Li_2BeF_4 system [12], improving the accuracy of calculation.

In this paper, instead of adopting IPMD with the interatomic potentials, FPMD is employed to enhance our knowledge of ionic micro-structure and transport properties of KF-NaF-AlF_3-Al_2O_3 system directly. Firstly, details of computational method to simulate the system

* Corresponding author.
E-mail address: csu13574831278@csu.edu.cn (H. Zhang).

https://doi.org/10.1016/j.jfluchem.2020.109546
Received 29 October 2019; Received in revised form 22 April 2020; Accepted 28 April 2020
Available online 04 May 2020

Table 1
Molecular dynamics simulation conditions.

CR_t	Al_2O_3 %.mol	N_K	N_{Na}	N_{Al}	N_F	N_O	N_{total}	Volume(Å^3)
1.3	1	29	9	31	125	3	197	4173.28
1.3	2	29	8	33	124	6	200	4370.72
1.3	3	29	7	34	120	9	199	4427.10
1.3	4	29	6	35	116	12	198	4492.13
1.3	5	29	6	36	113	15	199	4574.29
1.3	6	29	5	38	112	18	202	4657.46

by FPMD are illustrated. In the results and discussion section, the ionic micro-structure and transport properties are calculated and compared with the experimental values to test our FPMD model. The calculation results in this paper can provide a useful guide for designing suitable electrolyte system in aluminum electrolysis production.

2. Computational methods

2.1. Details of molecular dynamics simulation

The chemical composition of KF-NaF-AlF_3-Al_2O_3 (CR_t([KF] + [NaF])/[AlF_3]) = 1.3) system simulated by FPMD and the volume of the simulation box are shown in Table 1. The initial calculation models are obtained by randomly dropping ions into designated size boxes by Packmol software [22]. The density of the simulation boxes are set to 1.66–1.82 g/cm^3. For lacking of experimental values on the density of KF-NaF-AlF_3-Al_2O_3 system, data in this part are calculated by FactSage thermodynamic software [23]. FPMD calculations are carried out by adopting CASTEP module [24] and Perdew-Burke-Ernzerhof(PBE) exchange-correlation function in the generalized gradient approximation (GGA) [21]. Ultrasoft pseudo potentials(USPP) [8] have been employed for all the ion-electron interactions, where Na2s^{2}2p^{6}3s^1, Al3s^{2}3p^1, K3s^{2}3p^{6}4s^1, F2s^{2}2p^5 and O2s^{2}2p^4 electrons are regarded as valence electrons. DFT-D2 method is applied to dispersion correction to improve calculation accuracy [17]. FPMD uses 520 eV [8] cut-off energy and 2 *2 *2 k-point grid. Periodic boundary conditions are employed in the simulation boxes to eliminate the influence of boundary effect, making the results more reliable. FPMD simulation uses NVT ensemble (fixed number of particles, volume and temperature) with the Nosé-thermostat, and the temperature is set to 1150 K [25]. To obtain more accurate ionic micro-structure and transport properties, the systems are simulated in 5000 steps under NVT ensemble to obtain the ionic structure close to the real system, and then the structure relaxations are carried out in 10,000 steps. The simulation time steps are set to 1 fs and the total simulation time are 15 ps. It is noteworthy that Amelia Bengtson [17] points out that 216 ions and 6 − 12 ps for melt is enough to obtain a good agreement with the experimental results. The final 10,000 frames of particle trajectory information are collected to analyze the ionic micro-structure and transport properties of KF-NaF-AlF_3-Al_2O_3 system.

2.2. Statistical method of structural information

Radial distribution function (RDF) is an important method to describe liquid structure [7,8]. Extracted from molecular dynamics simulation trajectory, RDF can analyze the local ionic structure of fluoride melt, implying the probability that another particle will appear within the radius Δr with the particle at the r position as the center, as is shown in Eq. (1).

$$g_{ij}(r) = \frac{V}{N_i N_j} \sum_j \left\langle \frac{n_{ij}(r, \Delta r)}{4\pi r^2} \right\rangle \quad (1)$$

Where V is the volume of simulation box, N is the number of particles, $n_{ij}(r, \Delta r)$ is the average number of ion j surrounding a central ion i within a defined cut-off distance Δr.

The first shell coordination number (CN) of F ions around Al ion can be obtained by numerical integration of RDF within a certain cut-off radius, corresponding to the first minimum radius [21].

$$N_{Al-F} = 4\pi\rho_F \int_0^R r^2 g_{Al-F}(r) dr \quad (2)$$

Where $g_{Al-F}(r)$ is the RDF of Al-F, ρ_F is the average density of F ions and R is the cut-off radius.

Meanwhile, based on the particle trajectory data obtained by FPMD, the distribution of F, O ion, Al-F complex ion groups and the bond angle distribution of Al-O-Al and F-Al-F configuration are calculated. All the calculations are completed by MATLAB software.

2.3. Calculation of transport properties

Transport properties of KF-NaF-AlF_3-Al_2O_3 system is very significant for aluminum electrolysis process. Through analyzing particle trajectory data produced by FPMD, the self-diffusion coefficient of ions in the system are obtained according to the following equations [8].

$$MSD = \langle \Delta \bar{r}(t)^2 \rangle = \frac{1}{N} \langle \sum |r_{i(t)} - r_{i(0)}|^2 \rangle \quad (3)$$

$$D = \lim_{t\to\infty} \frac{1}{6} \frac{d[\Delta r(t)^2]}{dt} \quad (4)$$

Where $r_{i(t)}$ is the position of ion i at t moment, $< >$ is the statistical average value of the ensemble, N is the number of ions, MSD is mean square displacement and D is self-diffusion coefficient of ions.

The viscosity η and ionic conductivity σ can be obtained by combining the self-diffusion coefficient D with the Einstein–Stokes equation and Nernst-Einstein equation, respectively [15].

$$\eta = \frac{K_B T}{D\lambda} \quad (5)$$

$$\sigma = D\frac{nq^2}{K_B T} \quad (6)$$

Where K_B is the Boltzmann constant, which equals to 1.38×10^{-23}J/K. T is the temperature of the system, λ is the step length of ion diffusion, n is the unit volume concentration of ions and q is the charge of ion.

3. Results and discussion

3.1. Micro-structure

The micro-structure of KF-NaF-AlF_3-Al_2O_3 system simulated by FPMD is shown in Fig. 1, from which K and Na ions are randomly distributed in the simulation box, and the distance between ions is large because of small polarity differences of K-K, K-Na and Na-Na ions, and there is no covalent characteristic. The ionic micro-structures in the simulation box are dominated by four-coordinated $[AlF_4]^-$, five-coordinated $[AlF_5]^{2-}$ and six-coordinated $[AlF_6]^{3-}$ complex ion groups, which corresponds to distorted tetrahedron, triangular bipyramid and octahedron configurations, respectively. Meanwhile, due to the existence of bridge F ions and bridge O ions, these Al-F complex ion groups form more intricate spatial configuration. Although KF-NaF-AlF_3-Al_2O_3 system loses its long-range ordered state, the local ionic structure remains the short-range ordered state.

3.2. Radial distribution function

RDF of different ion pairs in KF-NaF-AlF_3-Al_2O_3 system is shown in Fig. 2. After $r > 6$ Å, g(r) values of different ion pairs gradually approach 1, which is consistent with the short-range ordered and long-range disordered structure of the system. The first peak value of RDF of Al-O and Al-F ion pairs is high and sharp, which means that the binding

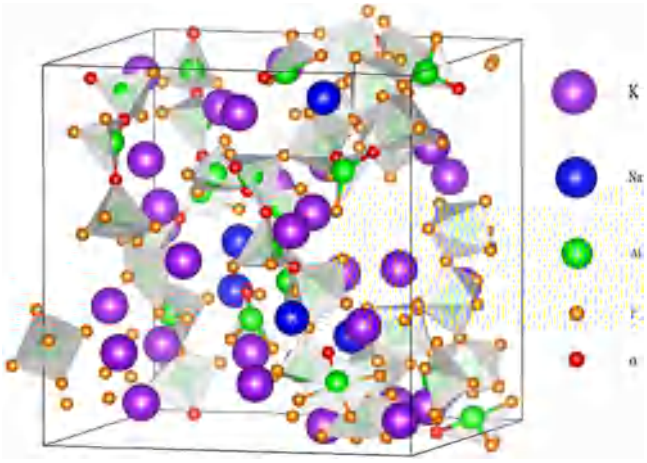

Fig. 1. The stable configuration of KF-NaF-AlF_3-Al_2O_3 system (Al_2O_3 mol.% = 6).

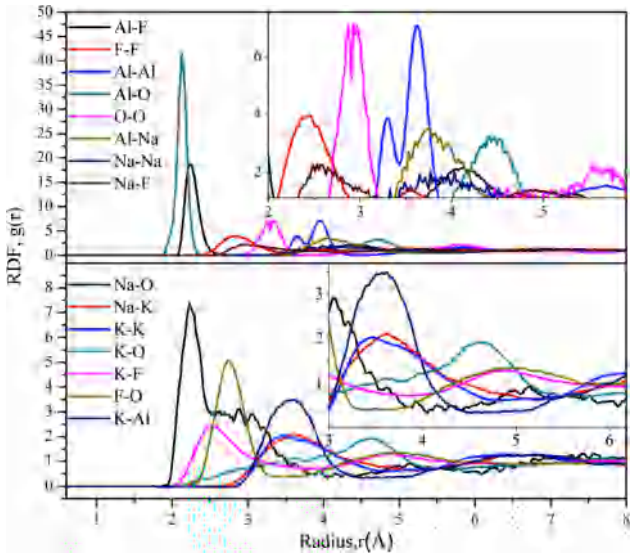

Fig. 2. Radial distribution function of different ion pairs in KF-NaF-AlF_3-Al_2O_3 system (Al_2O_3 mol.% = 6).

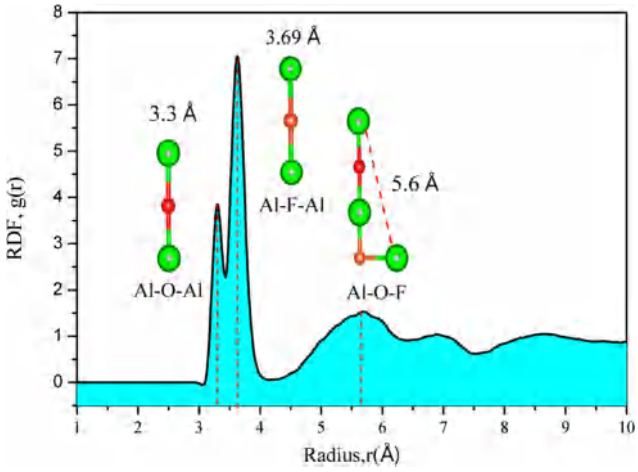

Fig. 3. Radial distribution function of A-Al ion pair (Al_2O_3 mol.% = 6).

ability of O and F ions with Al ions in melt is strong and Al-O-F complex ion groups are easily formed. In general, the first peak radius of RDF represents the average bond length of an ion pair, as is shown in Table 2. The average bond length of different ion pairs calculated in this paper are in good agreement with the previous research [8,26], and the change of Al_2O_3 concentration has little effect on the average bond length of ion pairs. The average bond length of Al-O is 1.61–1.65 Å, slightly less than that of Al-F ion pair, and the g(r) value of Al-O is much higher than that of Al-F, which shows the binding ability of O to Al is slightly stronger than that of F to Al [1].

On the whole, RDF curve of Al-Al ion pair can reflect polymerization degree of KF-NaF-AlF_3-Al_2O_3 system, because F and O ions may act as bridge ions to connect two Al ions to form more intricate spatial configurations. RDF curve of Al-Al ion pair is shown in Fig. 3. There are three obvious peaks on RDF curve of Al-Al ion pair, which are located at 3.3 Å, 3.6 Å and 5.6 Å. The peak at 3.3 Å is just twice of the first peak radius of the Al-O ion pair, which corresponds to the Al-O-Al configuration in melt, and the O ion acts as a bridge ion to connect two Al ions. The main peak occurs at about 3.6 Å, which is just twice of the first peak radius of Al-F ion pair, indicating that most F ions are connected to two Al ions as bridge ions. The peak at 5.6 Å corresponds to Al-O-F complex ion groups. In summary, there are not only simple $[AlF_4]^-$, $[AlF_5]^{2-}$ and $[AlF_6]^{3-}$ complex ion groups, but also intricate ionic configurations formed for the presence of bridge O and bridge F ions in KF-NaF-AlF_3-Al_2O_3 system.

Table 2
The average bond length(Å) of ion pairs and the average CN of Al-F ions in KF-NaF-AlF_3-Al_2O_3 system.

	Ion pair	1 mol.%	2 mol.%	3 mol.%	4 mol.%	5 mol.%	6 mol.%	Ref
Bond length (Å)	Al-F	1.77	1.75	1.77	1.79	1.77	1.81	1.82[a]
	F-F	2.49	2.51	2.51	2.53	2.53	2.51	2.51[a]
	Al-Al	3.67	3.69	3.69	3.67	3.67	3.69	3.61[b]
	Na-Na	3.73	3.73	3.75	3.73	3.75	3.73	3.65[b]
	Na-Al	3.75	3.73	3.65	3.71	3.73	3.67	3.59[a]
	Na-F	2.41	2.45	2.43	2.47	2.43	2.43	2.21[a]
	K-Al	3.51	3.55	3.59	3.57	3.57	3.55	3.49[b]
	K-Na	3.51	3.53	3.53	3.55	3.55	3.57	3.73[b]
	K-F	2.51	2.57	2.51	2.51	2.53	2.53	2.63[b]
	K-K	3.47	3.41	3.53	3.57	3.43	3.45	
	Al-O	1.65	1.63	1.61	1.65	1.63	1.63	1.60[a]
	Na-O	2.25	2.27	2.25	2.29	2.29	2.31	2.35[a]
	K-O	4.61	4.59	4.53	4.57	4.57	4.59	
	F-O	2.71	2.79	2.73	2.71	2.73	2.71	2.69[a]
	O-O	2.87	2.89	2.93	2.97	2.95	2.95	2.94[a]
CN	Al-F	5.31	5.35	5.40	5.42	5.43	5.45	5.71[a]

[a] Ref. [26].
[b] Ref. [8].

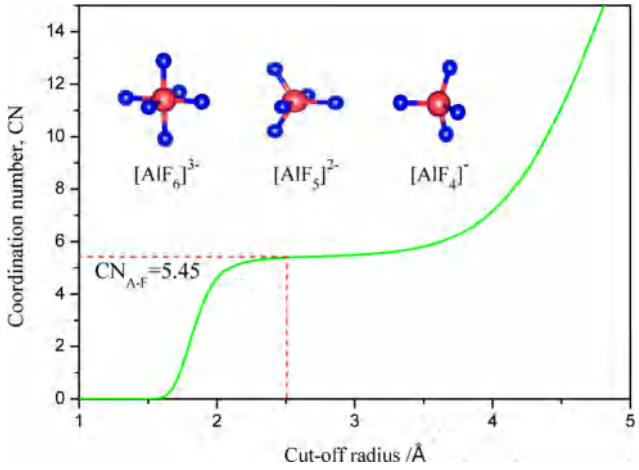

Fig. 4. Average CN integral curve of Al-F ion pairs (Al_2O_3 mol.% = 6).

3.3. Coordination number

The average CN of Al-F complex ion groups in KF-NaF-AlF_3-Al_2O_3 system can be obtained by integrating RDF curves. The average CN integral curve of Al-F complex ion groups is shown in Fig. 4 (Al_2O_3 mol. % = 6). When the cut-off radius is 2.5 Å, the average CN is 5.45. The average CN with different Al_2O_3 concentrations can also be obtained by integration, as is shown in Table 2. The average CN is between 5 and 6, which indicates that $[AlF_4]^-$, $[AlF_5]^{2-}$ and $[AlF_6]^{3-}$ coexist in the system. With the increasing concentration of Al_2O_3, the average CN also increases gradually, implying Al-F complex ion groups are gradually transformed into complex ion groups with higher CN.

3.4. Bond angles distributions

In this paper, the bond angle distribution of F-Al-F and Al-O-Al in KF-NaF-AlF_3-Al_2O_3 system is calculated, as is shown in Fig. 5. The ideal $[AlF_6]^{3-}$ octahedron has eight 90° and three 180 °F-Al-F bond angles; the ideal $[AlF_5]^{2-}$ triangular bipyramid has six 90°, three 120° and one 180 °F-Al-F bond angles; and the ideal $[AlF_4]^-$ regular tetrahedron has six 109.5 °F-Al-F bond angles [21]. From Fig. 5(a), the peak value of the bond angle distribution curve of F-Al-F is mainly located near 90° and 180°, corresponding to the Al-F complex ion structure of an octahedron or triangular bipyramid, respectively. Meantime, a small peak is found at about 110°, which corresponds to the tetrahedral Al-F complex ion group. However, this peak disappears gradually with the increase of Al_2O_3 concentration, which means that when Al_2O_3 concentration increases, the $[AlF_4]^-$ complex ion groups decrease gradually and transform into higher coordination complex ion groups. The calculated results of bond angle of F-Al-F configuration are consistent with average CN of the distribution of Al-F complex ion group. However, the positions of these peaks slightly deviate from their standard bond angles in ideal configurations, suggesting that the complex ion structures are distorted under melting conditions. Fig. 5(b) is the bond angle distribution of Al-O-Al, the peak value of bond angle distribution of Al-O-Al is about 170°, which is not affected by the concentration of Al_2O_3. This means bridge O ions connect two Al ions almost in a straight line, indirectly increasing the volume of complex ion groups. Based on the analysis of the bond angle distribution of F-Al-F and Al-O-Al, it can be concluded that the complex ion groups in KF-NaF-AlF_3-Al_2O_3 system are mainly composed of six-coordinated $[AlF_6]^{3-}$ and five-coordinated $[AlF_5]^{2-}$ ions. When the concentration of Al_2O_3 is low, there are a few four-coordinated $[AlF_4]$- complex ion groups in the melt while most of the complex ion groups do not exist alone, but are connected by bridge O and bridge F ions to form larger complex ion groups, which has been reflected in the calculation of RDF.

3.5. Distribution of Al-F complex ion groups, F and O ions type

In this paper, the distribution of Al-F complex ion groups in KF-NaF-AlF_3-Al_2O_3 system is calculated, as is shown in Fig. 6(a). With the increasing concentration of Al_2O_3, the proportion of $[AlF_6]^{3-}$ and $[AlF_5]^{2-}$ increases gradually, while the proportion of $[AlF_4]^-$ decreases gradually and keeps a low level. When the concentration of Al_2O_3 is more than 4%, the proportion of $[AlF_5]^{2-}$ decreases gradually, which is consistent with the change of average CN of Al-F complex ion groups. F ion and O ion types (Bridge fluorine F_b, F ion connects two Al

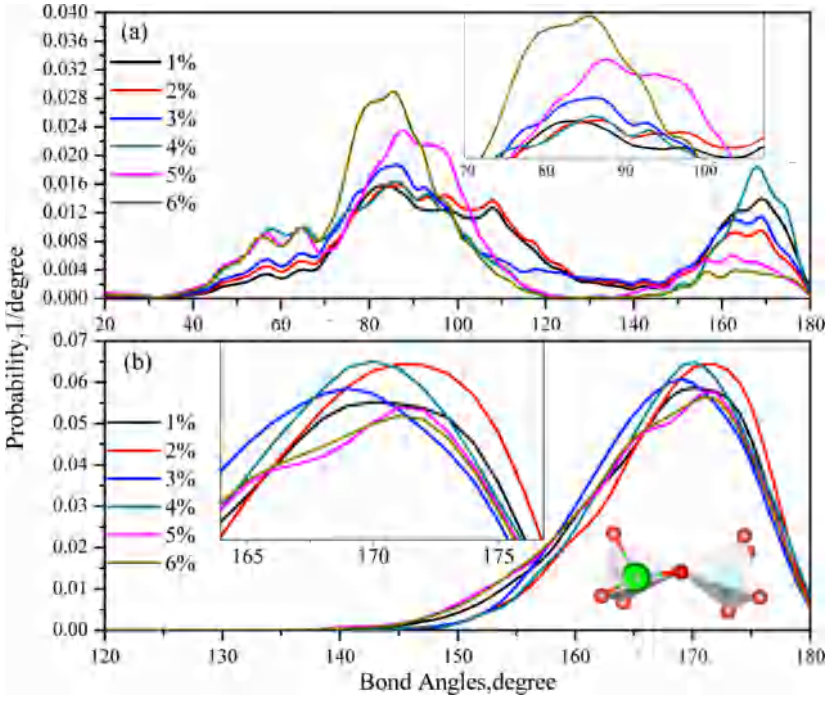

Fig. 5. Bond angle distribution of F-Al-F and Al-O-Al in KF-NaF-AlF_3-Al_2O_3 system, (a) F-Al-F; (b) Al-O-Al.

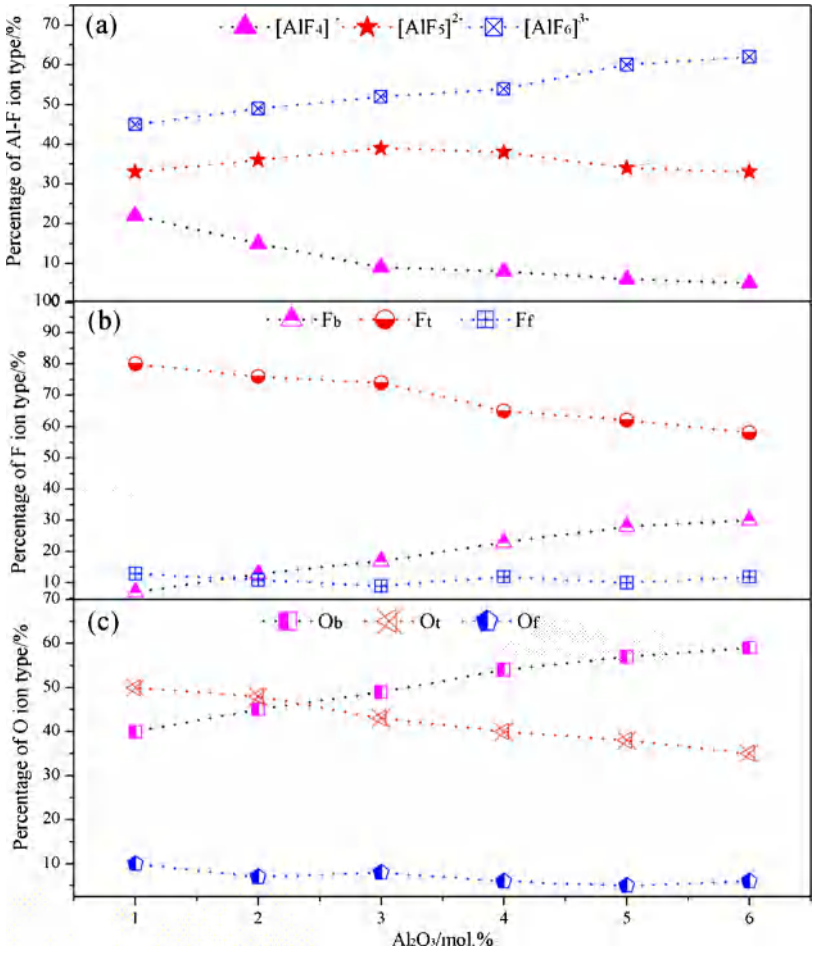

Fig. 6. Distribution of Al-F complex ion groups, F and O ions type, (a) Al-F complex ion groups; (b) F ions type; (c) O ions type.

ions in the form of Al-F-Al; terminal fluorine F_t, F ion connects with a neighboring Al ion and free fluorine F_f, F ion does not interact with neighboring Al ions. Similarly, O_b, O_t, O_f denote bridge oxygen, terminal oxygen and free oxygen ion, respectively) determines the polymerization degree of ionic structure and exerts a crucial impact on the transport properties of the system. Fig. 6(b) and (c) show the distribution of F and O ions in the melt. With the increasing concentration of Al_2O_3, the concentration of F_b and O_b increases gradually but the concentration of F_t and O_t ions decreases gradually, while the concentration of F_f and O_f ions maintains at a lower level. The higher concentration of F_b and O_b makes the Al-F complex ions form larger volume complex ion groups. The diffusion of these larger volume complex ions in the electrolyte will inevitably be affected by each other's spatial configuration and become intricate. Meanwhile, it can be clearly seen that the proportion of O_b ions is much higher than that of F_b ions, because the binding ability of O ions to Al ions is stronger than that of F ions, which is consistent with the calculated results of RDF.

3.6. Transport properties

Transport properties of KF-NaF-AlF_3-Al_2O_3 system is very important for aluminium electrolysis process. Fig. 7 shows MSD curves of different ions in the system in which the ions in the melt basically reach free diffusion state during the simulation time of 5−15 ps, indicating the whole FPMD simulation process is close to the equilibrium state [7]. According to MSD curves of different ions, the self-diffusion coefficients of ions can be calculated. From Fig. 8, the diffusion ability of different ions in the melt is Na > K > F > O > Al. The strong diffusion ability of Na and K ions implies that they do not form intricate complex ion

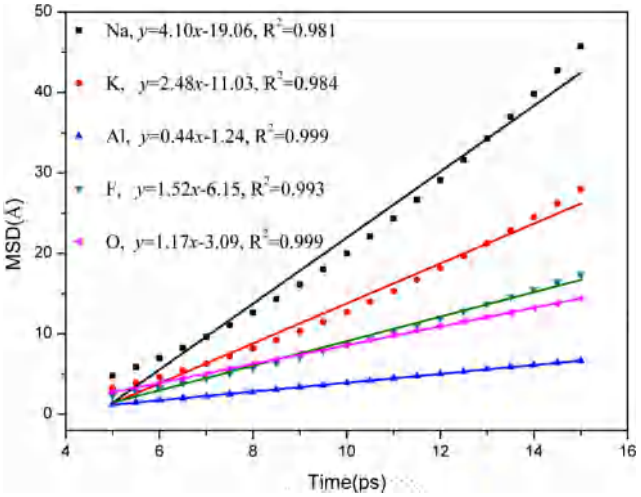

Fig. 7. MSD curves of ions in KF-NaF-AlF_3-Al_2O_3 system.

groups with the main F and O anions, but are randomly distributed in the whole system with a free diffusion state, and their diffusion ability is slightly lower than that of Na ions because of larger volume and mass of K ions. However, the diffusion ability of Al, F and O ions is weak, because of large polarity difference between Al ions, F ions and O ions, and intricate complex ion groups are easily formed. With the increasing concentration of Al_2O_3, the self-diffusion coefficients of different ions in the system decrease due to the existence of F_b and O_b and a larger volume of Al-F-Al and Al-O-Al complex ion groups are formed, making

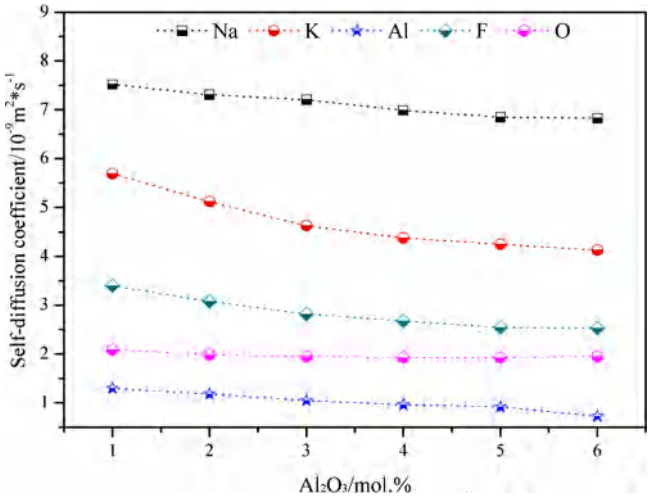

Fig. 8. Self-diffusion coefficients of ions in KF-NaF-AlF_3-Al_2O_3 system.

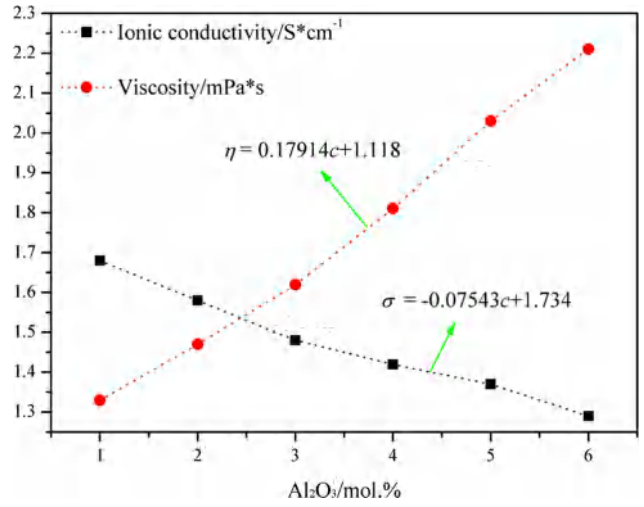

Fig. 9. Ionic conductivity and viscosity of KF-NaF-AlF_3-Al_2O_3 system.

the diffusion of ions more difficult.

In this paper, the ionic conductivity and viscosity of KF-NaF-AlF_3-Al_2O_3 system are calculated, as is shown in Fig. 9. At present, relevant experimental data are scarce due to the high temperature and strong corrosion characteristics of aluminum electrolyte. The ionic conductivity of the melt is calculated from 1.2 to 1.7 S/cm and decreases with the increase of Al_2O_3 concentration, which is much smaller than that in the conventional NaF-AlF_3 system(2.8 S/cm) [23]. On the one hand, the melting point of KF-NaF-AlF_3-Al_2O_3 system is lower than that of the conventional NaF-AlF_3 system. On the other hand, the ionic structure of the system becomes more intricate due to the addition of Al_2O_3, reducing the self-diffusion coefficient of ions and ionic conductivity. Moreover, the ionic conductivity of the system calculated by FPMD is 1.2–1.7 S/cm, which is partly in line with the experimental values of 1.0–1.5 S/cm with ([KF] + [NaF])/[AlF_3] = 1.3–1.5 between 700 − 800 ℃ [27], 1.29–1.46 S/cm with ([KF] + [NaF])/[AlF_3] = 1.3–3.0 between 740 − 800 ℃ [28]. The deviation between the calculated value and experimental value attributes to the different molecular ratio, temperature and the addition of Al_2O_3. The calculation results of viscosity for KF-NaF-AlF_3-Al_2O_3 system are between 1.3 and 2.2 mPa*s, and the viscosity of the system increases with the increasing concentration of Al_2O_3. The ionic conductivity and viscosity vary linearly with the concentration of Al_2O_3, so the function relationship between ionic conductivity, viscosity and the concentration of Al_2O_3 is fitted as follows.

$$\sigma = -0.07543c + 1.734 \quad (7)$$

$$\eta = 0.17914c + 1.118 \quad (8)$$

Where σ is ionic conductivity, η is viscosity and c is the concentration of Al_2O_3. Although the experimental data on the viscosity and ionic conductivity of the system are scarce, relatively reasonable results can be obtained by FPMD simulation.

4. Conclusions

In this paper, the ionic micro-structure and transport properties of KF-NaF-AlF_3-Al_2O_3 system are calculated by FPMD method. The results show that the complex ion groups in it are mainly $[AlF_5]^{2-}$ and $[AlF_6]^{3-}$, while $[AlF_4]^-$ are few. The average CN of Al-F complex ion groups is between 5 and 6 and it increases gradually with the increasing concentration of Al_2O_3. The binding ability of O and F ions with Al ions in the melt is strong, O and F ions connect Al ions in the form of bridge ions to form more intricate Al-F-Al, Al-O-Al and Al-O-F complex ion groups. The diffusion ability of ions in the system is Na > K > F > O > Al. With the increasing concentration of Al_2O_3, the ionic conductivity decreases but the viscosity increases gradually, which is consistent with the changing rule of ionic structure. Meanwhile, the functional relationship between ionic conductivity, viscosity and Al_2O_3 concentration is fitted. In aluminum electrolysis industry, the dissolution and transport of alumina in electrolytes is very important. The changes of ion structure and transport properties of KF-NaF-AlF_3-Al_2O_3 system with different alumina concentrations are studied in this paper, which will have a positive effect on industrial production and point out the research direction for new low-temperature aluminum electrolytes.

Declaration of Competing Interest

The authors declare that they have no known competing financial interests or personal relationships that could have appeared to influence the work reported in this paper.

Acknowledgments

This work was financially supported by the National Natural Science Foundation of China (51974373, 51874365, 51674300, 61751312, and 61621062), the Major Scientific and Technological Innovation Projects of Shandong Province (2019JZZY020123), the Natural Science Foundation of Hunan Province, China (2018JJ2521), the Fundamental Research Funds for the Central Universities of Central South University (CX20190195). We sincerely acknowledge the software support of Shenzhen Supercomputing Center.

References

[1] K. Machado, D. Zanghi, M. Salanne, V. Stabrowski, C. Bessada, Anionic structure in molten cryolite-alumina systems, J. Phys. Chem. C 122 (2018) 21807–21816, https://doi.org/10.1021/acs.jpcc.8b06905.
[2] B. Kubíková, J. Mlynáriková, M. Boča, Z. Shi, B. Gao, N. Patel, Temperatures of primary crystallization and density of the KF + AlF_3 + LiF + Al_2O_3 molten system, J. Chem. Eng. Data 63 (2018) 3047–3052, https://doi.org/10.1021/acs.jced.8b00157.
[3] H. Yan, J. Yang, W. Li, Surface tension and density in the KF-NaF-AlF_3-based electrolyte, J. Chem. Eng. Data 56 (2011) 4147–4151, https://doi.org/10.1021/je2005825.
[4] V. Danielik, J. Gabčová, Phase diagram of the system NaF-KF-AlF_3, J. Therm. Anal. Calorim. 76 (2004) 763–773, https://doi.org/10.1023/B:JTAN.0000032261.54207.1e.
[5] R. Chen, G. Wu, Q. Zhang, Phase diagram of the system KF-AlF_3, J. Am. Ceram. Soc. 83 (2000) 3196–3198, https://doi.org/10.1111/j.1151-2916.2000.tb01703.x.
[6] A. Apisarov, A. Dedyukhin, E. Nikolaeva, P. Tinghaev, O. Tkacheva, A. Redkin, Y. Zaikov, Liquidus temperatures of cryolite melts with low cryolite ratio, Metall. Mater. Trans. B 42 (2011) 236–242, https://doi.org/10.1007/s11663-010-9462-5.
[7] H. Guo, J. Li, H. Zhang, T. Li, J. Luo, X. Yu, S. Wu, C. Zong, First-principles molecular dynamics investigation on KF-NaF-AlF_3 molten salt system, Chem. Phys.

Lett. 730 (2019) 587–593, https://doi.org/10.1016/j.cplett.2019.06.060.
[8] X. Lv, Z. Han, H. Zhang, Q. Liu, J. Chen, L. Jiang, Ionic structure and transport properties of KF-NaF-AlF_3 fused salt: a molecular dynamics study, Phys. Chem. Chem. Phys. 21 (2019) 7474–7482, https://doi.org/10.1039/C9CP00377K.
[9] Z. Akdeniz, P.A. Madden, Raman spectra of ionic liquids: a simulation study of AlF_3 and its mixtures with NaF, J. Phys. Chem. B 110 (2006) 6683–6691, https://doi.org/10.1021/jp060064h.
[10] C. Bessada, A. Rakhmatullin, A.L. Rollet, D. Zanghi, High temperature NMR approach of mixtures of rare earth and alkali fluorides: An insight into the local structure, J. Fluorine. Chem. 130 (2009) 45–52, https://doi.org/10.1016/j.jfluchem.2008.07.010.
[11] V. Cristiglio, L. Hennet, G.J. Cuello, M.R. Johnson, A. Fernández-Martínez, H.E. Fischer, I. Pozdnyakova, D. Zanghi, S. Brassamin, J.-F. Brunb, D.L. Price, Ab-initio molecular dynamics simulations of the structure of liquid aluminates, J. Non-Cryst. Solids 353 (2007) 1789–1792, https://doi.org/10.1016/j.jnoncrysol.2007.01.075.
[12] A. Klix, A. Suzuki, T. Terai, Study of tritium migration in liquid Li_2BeF_4 with ab initio molecular dynamics, Fusion Eng. Des. 81 (2006) 713–717, https://doi.org/10.1016/j.fusengdes.2005.09.034.
[13] R.D. Banhatti, A. Heuer, Structure and dynamics of lithium silicate melts: molecular dynamics simulations, Phys. Chem. Chem. Phys. 3 (2001) 5104–5108, https://doi.org/10.1039/B106013A.
[14] K. Machado, D. Zanghi, M. Salanne, C. Bessada, Structural, dynamic, and thermodynamic study of KF-AlF_3 melts by combining high-temperature NMR and molecular dynamics simulations, J. Phys. Chem. C 123 (2019) 2147–2156, https://doi.org/10.1021/acs.jpcc.8b11907.
[15] T. Wu, S. He, Y. Liang, Q. Wang, Molecular dynamics simulation of the structure and properties for the CaO-SiO_2 and CaO-Al_2O_3 systems, J. Non-Cryst. Solids 411 (2015) 145–151, https://doi.org/10.1016/j.jnoncrysol.2014.12.030.
[16] R. Car, M. Parrinello, Unified approach for molecular dynamics and density-functional theory, Phys. Rev. Lett. 55 (1985) 2471–2474, https://doi.org/10.1103/PhysRevLett.55.2471.
[17] A. Bengtson, H.O. Nam, S. Saha, R. Sakidja, D. Morgan, First-principles molecular dynamics modeling of the LiCl-KCl molten salt system, Comp. Mater. Sci. 83 (2014) 362–370, https://doi.org/10.1016/j.commatsci.2013.10.043.
[18] C. Kwon, J. Kang, W. Kang, D. Kwak, B. Han, First principles study of the thermodynamic and kinetic properties of U in an electrorefining system using molybdenum cathode and LiCl-KCl eutectic molten salt, Electrochim. Acta 195 (2016) 216–222, https://doi.org/10.1016/j.electacta.2016.02.123.
[19] C. Kwon, J. Kang, B. Han, First-principles based computational study on nucleation and growth mechanisms of U on Mo(110) surface solvated in an eutectic LiCl-KCl molten salt, Int. J. Energ. Res. 40 (2016) 1381–1388, https://doi.org/10.1002/er.3527.
[20] C. Kwon, S.H. Noh, H. Chun, I.S. Hwang, B. Han, First principles computational studies of spontaneous reduction reaction of Eu (III) in eutectic LiCl-KCl molten salt, Int. J. Energ. Res. 42 (2018) 2757–2765, https://doi.org/10.1002/er.4064.
[21] X. Lv, Z. Xu, J. Li, J. Chen, Q. Liu, First-principles molecular dynamics investigation on Na_3AlF_6 molten salt, J. Fluorine. Chem. 185 (2016) 42–47, https://doi.org/10.1016/j.jfluchem.2016.03.004.
[22] L. Martínez, R. Andrade, E.G. Birgin, J.M. Martínez, PACKMOL: a package for building initial configurations for molecular dynamics simulations, J. Comput. Chem. 30 (2009) 2157–2164, https://doi.org/10.1002/jcc.21224.
[23] C.W. Bale, P. Chartrand, S.A. Degterov, G. Eriksson, K. Hack, R.Ben. Mahfoud, J. Melancon, A.D. Pelton, S. Petersen, FactSage thermochemical software and databases, Calphad 26 (2002) 189–228, https://doi.org/10.1016/S0364-5916(02)00035-4.
[24] S.J. Clark, M.D. Segall, C.J. Pickard, P.J. Hasnip, M.I. Probert, K. Refson, M.C. Payne, First principles methods using CASTEP, Z. Kristallogr. 220 (2005) 567–570, https://doi.org/10.1524/zkri.220.5.567.65075.
[25] V.N. Nekrasov, O.V. Limanovskaya, A.V. Suzdal'tsev, A.P. Khramov, Y.P. Zaikov, Stationary anodic process at platinum in KF-NaF-AlF_3-Al_2O_3 melts, Russ. Metall (Metally). (2014) 664–670, https://doi.org/10.1134/S0036029514080084.
[26] D.K. Belashchenko, O.I. Ostrovski, S.Y. Saposznikova, Computer study of structure, thermodynamic, and electrical transport properties of Na_3AlF_6-Al_2O_3 and CaF_2-Al_2O_3 melts, Metall. Mater. Trans. B 29 (1998) 105–110, https://doi.org/10.1007/s11663-998-0012-3.
[27] A. Dedyukhin, A. Apisarov, O. Tkacheva, A.A. Redkin, Y. Zaikov, A. Frolov, A. Gusev, Electrical conductivity of the (KF-AlF_3)-NaF-LiF molten system with Al_2O_3 additions at low cryolite ratio, ECS Trans. 16 (2009) 317–324, https://doi.org/10.1149/1.3159336.
[28] A.P. Apisarov, A.E. Dedyukhin, A.A. Red'kin, O.Y. Tkacheva, Y.P. Zaikov, Physicochemical properties of KF-NaF-AlF_3 molten electrolytes, Russ. J. Electrochem +. 46 (2010) 633–639, https://doi.org/10.1134/S1023193510060066.